Functional organic adlayers for controlling the adhesion strength of electrolessly deposited copper on super-engineering plastics

Hugo Nolan, Federico Zen, Alican Gençer, Lua Henderson, Martin Kelly, Filippo Pota, Christian Schröder, Eoin M. Scanlan, Paula E. Colavita[*]

a- School of Chemistry, Trinity College Dublin, College Green, Dublin 2, Ireland

[*] Corresponding author email: colavitp@tcd.ie

Abstract

Effective metallization of super-engineering plastics such as liquid crystal polymers (LCP) and polyphenylene sulfides (PPS) via electroless deposition of copper thin films is an important step in the manufacturing of a wide range of devices. Copper deposition typically requires a pre-treatment step involving chemical and/or mechanical roughening to ensure high adhesion at the polymer/Cu interface; however such treatments are detrimental to patterns and topographic features of the polymer that possess μm resolution and/or high aspect ratio. Herein, we demonstrate that it is possible to regulate and improve adhesion of electrolessly deposited copper thin films at LCP and PPS materials via multilayer functionalization with aryldiazonium cations of a *p*-aminobenzoic acid precursor. We first demonstrate that aryldiazonium grafting conditions can be optimized to overcome the chemical inertness of LCP/PPS without resorting to harsh oxidative or mechanical treatments. We then show that the density of Ar-COOH groups can be regulated by modifying the number of functionalization cycles. X-ray photoelectron spectroscopy studies shows that this has a clear impact on the composition of the catalytic nanoparticle layer required for copper deposition. Adhesion strength studies demonstrate that such changes translate into improved adhesion strengths without any adverse effects on surface roughness. Control experiments with alternative chemical moieties suggest that specific chemical interactions between catalytic seeds and grafted carboxylate groups play an important role in the observed improved adhesion.

KEYWORDS: electroless; copper; metallization; polymers; adhesion; plating; diazonium

Introduction

Metallization of non-conductive polymers and their composites via electroless deposition has important applications in the semiconductor industry and generally in information and communication technologies [1, 2]. The metallization process aims at depositing a metal layer from solution through surface catalyzed reactions; typically, this electrolessly deposited layer is then used as a conductive contact for the subsequent electroplating of the same or a different metal. The properties of the electrolessly deposited layer are therefore essential for the successful fabrication of interconnects, cavities and other electronic components on polymeric supports at length scales that can vary from mm to nm [3].

A typical polymer metallization process via electroless deposition is shown in Figure 1a using copper as an example. First, a pre-treatment step, e.g. via chromic acid [1, 4], results in the creation of binding sites for sensitizer/activator species that catalyse electroless deposition. This step also oxidises and partially etches the polymer [4], leading to increased roughness that promotes mechanical adhesion of the metal layer to the substrate. Subsequently, the polymer undergoes sensitization/activation, e.g. via one- or two-step treatments with Sn(II) and Pd(II) solutions, yielding catalytic nanoparticles at the polymer surface [1, 4]. The surface might then be immersed in an acceleration bath to remove residual oxides and, finally, electroless deposition takes place, leading to metal growth. Several protocols for the preparation of solutions for sensitization, activation and deposition steps have been reported for various metals and substrates, as reviewed elsewhere [1, 2, 5, 6].

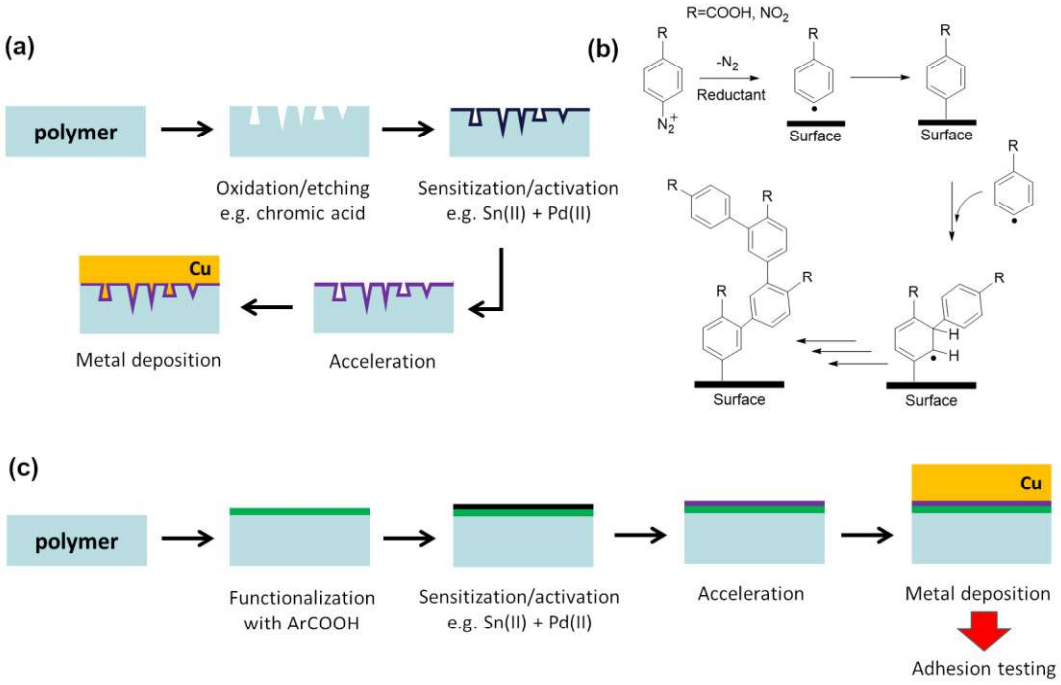

Figure 1. (a) Schematic description of a conventional electroless deposition process with copper as an example; the oxidative pre-treatment is shown to schematically result in "keying" or interlocking of the copper film and polymer substrate. (b) Surface modification using aryldiazonium cations via reductive formation of aryl radicals. The mechanism proposed for the formation of multilayers by Doppelt et al. is also shown [7]. (c) Schematic description of the copper electroless deposition protocol studied in this work, employing modification with ArCOOH groups via aryldiazonium cation reduction.

The pre-treatment step is essential to ensure strong metal adhesion and subsequent integrity and robustness of electroplated electronic components. Oxidized functionalities and formation of etched trenches during aggressive oxidation synergistically enhance adhesion through chemical interactions and mechanical 'keying' between the polymer and the metal [8, 9]. However, aggressive etching baths present significant problems as they can degrade polymer features whose dimensionality and/or aspect ratio are critical for applications. Furthermore, they involve environmentally harmful chemicals that present a problem of hazardous waste disposal and that are under high regulatory scrutiny [10]. For this reason, there has been great interest in replacing etching baths with strategies that enable control over final polymer substrate morphology and that address environmental concerns

associated with aggressive chemicals, while still delivering robust metal films. Among these, the use of functional surface layers is particularly attractive, as they can be in principle engineered to display strong chemical interactions with metal clusters and films, while also remaining conformal to the polymeric substrate.

Early studies on functionalization via acid nitration were reported by Rantell,[11] who showed that amino, diazo and hydroxylphenyl groups improved adhesion of electrolessly deposited copper to polystyrene. Both carboxylates and thio-groups have received attention as moieties that improve adhesion. Metz et al. demonstrated that molecular layers bearing -COOH groups obtained via UV-driven grafting could be used to both increase the rate of electroless deposition and to control the morphology of deposited metals (Au, Pt) at carbon fibers [12-14] due to improved density of binding sites for Sn(II) sensitizer species. Palacin and co-workers used self-assembled monolayers of dithiols to pattern the Pd^0 activator and, consequently, electrolessly deposited Cu features on Au surfaces with good adhesion [15]; while thiol-terminated adlayers prepared via UV silanization were used by Sawada et al. for Cu deposition on polyethyleneterephthalate (PET) [16]. Finally, thin functional polymeric brushes have been shown to simultaneously enhance activator loading and promote metal layer adhesion [17], through chemical adhesion and formation of interdigitated metal-polymer interfacial layers. For instance, Palacin and co-workers [18] used aryldiazonium salts to graft oligomers of polyacrylic acid (PAA), resulting in <15 nm thick carboxylate-rich layers that improved the adhesion of electrolessly deposited Ni and Cu onto ABS.

Although several functionalization routes have been investigated and shown to deliver improvements in adhesion, some of these are not applicable to polymers (e.g. self-assembled thiol layers). Also, while UV-, laser- and plasma-assisted surface modifications can be highly

effective on non-conductive substrates [19, 20], they are line-of-sight methods that are not amenable to the modification of complex geometries and can result in undesirable structural and chemical changes in polymers. Solution methods that use environmentally benign solvents/reactants are instead more attractive as they can be applied via flow, spray, immersion methods, and are applicable to inner surfaces and complex geometries.

In this work we report on a functionalization protocol from aqueous solution applicable to composite structural polymers, namely liquid crystal polymers (LCP) and polyphenylene sulfides (PPS), to achieve improved adhesion strength of electrolessly deposited copper layers. These polymers are considered super-engineering plastics [21] and are attractive for important and wide ranging applications that require metallization. We show for the first time that aryldiazonium chemistry can be used for the reductive functionalization of LCP and PPS (Figure 1b) with molecular adlayers. A study of Ar-COOH surface density on the sensitization-activation process and on the final copper adhesion strength was carried out (Figure 1c). We propose that aryldiazonium multilayer formation, which is typically thought to be an undesirable feature of this functionalization strategy [22-24], can be leveraged to achieve a degree of 'keying' at the nanoscale through a relatively mild and scalable solution-based process.

Experimental methods

Materials. *p*-aminobenzoic acid (99%), p-nitrobenzenediazonium tetrafluoroborate salt (pNBD, 97%), HCl (fuming, 36.5-38%), H_3PO_2 (50% w/w), $NaNO_2$ (99%), $CuSO_4 \cdot 5(H_2O)$ (>98%) and methanol (HPLC grade) were sourced commercially and used as received. A multistep Cu electroless deposition kit was obtained commercially (Circudep, Technic Inc. UK). All aqueous

solutions were prepared using deionized water. LCP and PPS substrates were sourced from FRD Science & Technology.

Diazotization and functionalization. The diazonium salt of the p-aminobenzoic acid (ABA) was prepared in aqueous solution by adapting previously published protocols [25, 26]. Briefly, ABA was first dissolved in 0.1 M HCl containing ca. 4% methanol (by vol.) to a final concentration of 18 mM; an 80 mM $NaNO_2$ stock solution was added dropwise until the concentrations of ABA and $NaNO_2$ were both 15 mM. This solution was then left for 1 h at 4 °C to allow for diazotization to take place. The 15 mM solution of the aryldiazonium salt (diazotized ABA or as received pNBD) were prepared immediately before functionalization reactions. For polymer modifications, $CuSO_4$ and hypophosphorous acid were added from concentrated stocks to the aryldiazonium solution to a final concentration of 5 mM and 0.5% (w/w), respectively. Polymer coupons were then immersed into this solution for 1 h, unless otherwise noted, then rinsed with water and methanol, dried and used for further characterization and/or metallization.

Electroless deposition. Electroless deposition followed the protocol provided by the manufacturer. Briefly, polymer coupons were first immersed in a pre-dip solution for 1 min (CIRCUDEP 1057 RTU); then for 5 min in a 3% solution of the Pd/Sn catalyst bath (CIRCUDEP 1055 B) in the pre-dip solution (sensitization/activation); then for 3 min in a 10% solution of the accelerator bath (CIRCUDEP 1060) in water (acceleration). Finally, the coupons were immersed in the copper electroless deposition bath (10% CIRCUDEP 1000 A and 10% CIRCUDEP 1000 B in water) which contained $CuSO_4$ (10-15%) and formaldehyde (5-13%) as reductant. Electroless deposition was carried out at 25 °C for 8 min, unless otherwise noted, which yields Cu thickness of ca. 0.5 µm according to the manufacturer's specifications.

Coupons used for adhesion strength tests were cut to size, mechanically cleaned using 50 nm alumina slurry (Buehler) on polishing cloths (MicroCloth®), then rinsed with water and methanol prior to functionalization and/or Cu deposition. Reference control samples with high adhesion Cu layers were obtained by following the above protocol but by preliminary sanding the LCP/PPS coupon using P1200 grit paper to achieve high roughness, as recommended by the manufacturer of the copper plating bath.

Characterization. Contact angles (CAs) were determined using the sessile drop method (FTA1000) using 2 µL droplets. Thermogravimetric analysis (TGA) was carried out in air at 10 °C/min using a Pyris 1 thermogravimetric analyzer (PerkinElmer) on 15-20 mg of sample shavings removed from the stock polymer coupons. Profilometry was carried out on a Dektak 6M instrument (Veeco). Fourier transform infrared (FTIR) absorption spectroscopy was carried out on an interferometer (Bruker T27) equipped with an N_2-cooled MCT detector and a hemispherical Ge attenuated total internal reflection crystal accessory (GATR, Harrick) at 4 cm^{-1} resolution. X-ray photoelectron spectroscopy (XPS) characterization was carried out in a UHV system at 1×10^{-10} mbar base pressure, equipped with a monochromatized Al K_α X-ray source (1486.6 eV) and a hemispherical analyzer. A neutralizer gun (CN10) was used for charge compensation. Spectra were baseline-corrected using a Shirley background and the energy scale was corrected using the C 1s peak energy as reference. Fits were carried out using commercial software (CasaXPS) and atomic percent compositions were determined by calculating peak area ratios after correction by relative sensitivity factors (RSF: C 1s = 1.0, N 1s = 1.8, O 1s = 2.93, Sn 3d = 25.05, Pd 3d = 16.04). Profilometry was carried out using a Dektak 6M instrument. Scanning electrochemical microscopy (SEM) was carried out on a Zeiss Ultra FE SEM. Adhesion strength was measured via peeling at 180° using a single column force tester (Mecmesin, MultiTest 2.5 dV). Coupons (5×2 cm^2) were mounted onto the sample

holder with double sided tape; a strip of test tape (Gorilla Tape®, steel adhesion rated at 1.24 N/mm) on the Cu layer was then peeled via a 100 mm displacement at 250 mm/min at a 180° angle (Figure S1). Peeling forces were then normalized by the width of the coupon to obtain adhesion strength values.

Results

Polymer characterization and surface functionalization

LCPs and PPS are partially crystalline polymers with high dimensional stability, strength and rigidity, good weatherability and high chemical inertness [27]. LCP has an aromatic polyester architecture based on hydroxybenzoic acid type of monomers and PPS is a polysulfide with typical repeat units as shown in Figure 2a. Both LCP and PPS are often manufactured as polymer blends containing reinforcing inorganic fibers [27]. Figures 2b and 2c display SEM images of LCP and PPS materials used, respectively, showing evidence of reinforcing fibers within the polymeric matrix. This was further confirmed via TGA in air, Figure 2c, which indicates that the inorganic content of the polymers used is *ca.* 40 wt.%. Infrared spectra in Figure 2d shows distinct spectral profiles for the two polymers. Peaks associated with the stretching mode of ester carbonyl peaks (ca. 1737 cm^{-1}) confirmed the presence of polyesters, while C—C skeletal stretching peaks (1470-1510 and 1600-1630 cm^{-1}) are consistent with the presence of aromatic rings [28, 29]. In the case of the PPS material used for experiments, the presence of the ester carbonyl peak indicates that the coupons consisted of a polymeric blend.

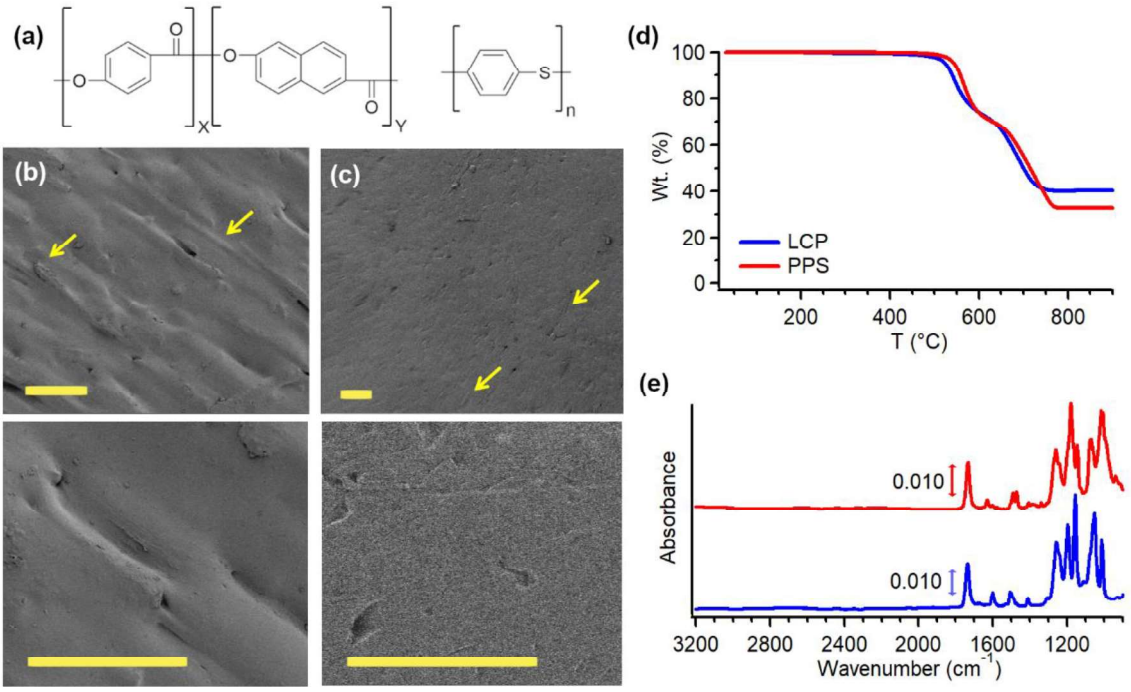

Figure 2. (a) Typical repeat units of LCP (left) and PPS (right) polymers. SEM images of (b) LCP and (c) PPS polymers (scalebar = 100 µm); arrows indicate examples of locations where reinforcing fibers are discernible in the images. (d) TGA curves in air for LCP and PPS polymers showing inorganic residues after oxidation. (e) FTIR spectra obtained via GATR for both LCP and PPS coupons used in our studies.

Functionalization with aryldiazonium cations has been demonstrated to take place on a range of polymers, as shown in work from our group [25, 30-33] and others [18, 34-37]. Grafting conditions can be tailored to covalently immobilize monomers or oligomers of the aryldiazonium precursor. In particular, if grafting occurs via formation of radicals in solution the aryldiazonium layer can grow into polyaryl multilayers as shown schematically in Figure 1b [7, 34, 36, 38, 39]. Similar S_H type reactions are proposed to be responsible for grafting onto polymers that bear aromatic rings in their backbone [25, 34]. Functionalization of LCP and PPS was therefore investigated on LCP and PPS using diazonium salts bearing carboxyphenyl (ABA) and nitrophenyl (pNBD) groups: carboxylates were of interest to promote binding of electrolessly deposited metals, whereas nitrophenyls were used as

diagnostic probes to monitor surface modifications via their strong -NO_2 absorptions [32]. The chemical inertness of the thermoplastic polymers used however presents a significant challenge to surface modification, particularly if aggressive oxidising treatments are to be avoided. Initial attempts at immobilization via simple immersion of coupons into aqueous solutions of aryldiazonium cations were indeed unsuccessful. Reductants such as iron ($E° = -0.447$ V) and hypophosphorous acid ($E°= -0.499$ V) have been reported to promote dediazoniation [37, 40-42]; among these we privileged use of hypophosphosphites as they can be applied in homogeneous solution thus facilitating processing and are frequently used in electroless deposition baths. Some degree of functionalization was observed spectroscopically (data not shown) when using relatively high concentrations (3 M) of H_3PO_2 in the aryldiazonium cation solution. However, best results were obtained by combining hypophosphite at lower concentration with addition of a Cu^{2+} salt [43, 44]. Figure 3a shows GATR infrared spectra of LCP and PPS before and after functionalization using 15 mM aqueous solutions of pNBD containing ca. 0.15 M hypophosphite and 5 mM Cu^{+2} (1 h reactions). Two peaks at 1524 and 1348 cm^{-1}, typically assigned to asymmetric and symmetric stretching modes of the -NO_2 group (indicated with arrows) [28, 32], become evident after the grafting procedure. This is also confirmed by the difference spectra, Figure 3b, which shows positive peaks at these two frequencies as well as a C—C stretching of -Ar groups at *ca.* 1600 cm^{-1}. Notably, these diagnostic peaks do not disappear after sonication in methanol (1 min), and their presence is not detected in the absence of H_3PO_2 as reductant, independently of the concentration of pNBD tested. This strongly suggests that the peaks are the result of covalent modification via formation of nitroaryl radical species from the diazonium cation.

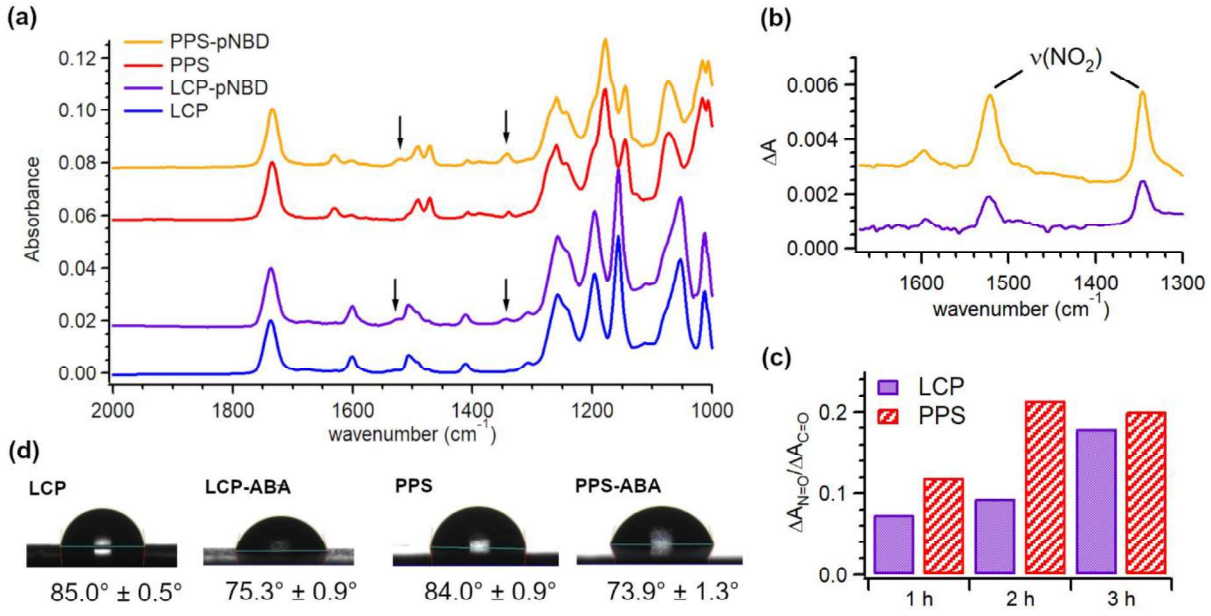

Figure 3. (a) GATR spectra of LCP and PPS substrates before and after functionalization for 1 h via immersion in a solution containing 15 mM pNBD, 0.1 M H_3PO_2 and 5 mM Cu^{+2}; spectra are shown stacked for clarity. (b) Difference absorbance spectra evidencing the presence of stretching modes of -NO_2 and -Ar groups in the GATR spectra of pNBD-functionalized PPS and LCP polymers; spectra are shown stacked for clarity. (c) Net absorbance ratios for the peaks at 1350 and 1735 cm^{-1} obtained at LCP and PPS surfaces after one, two and three repeated cycles of functionalization as in (a). (d) Water contact angle of LCP and PPS substrates before and after functionalization for 1 h via immersion in a solution containing 15 mM diazotized ABA, 0.1 M H_3PO_2 and 5 mM Cu^{+2}.

Shorter functionalization reactions (<1 h) resulted in low signals arising from NO_2-groups, hence shorter reaction times were not investigated spectroscopically. However, it was possible to monitor the effect of multiple functionalization steps on the density of surface nitrophenyl groups. Figure 3c shows the ratio between the net absorbances at 1348 and 1735 cm^{-1} ($\Delta I_{N=O}$ /$\Delta I_{C=O}$) after 1, 2 and 3 cycles of 1 h functionalization using pNBD as precursor. Use of ratios, rather than absolute peak absorbances, enables to account for differences in optical pathlength that arise from variations in coupon flatness or in pressure applied against the GATR optical element. Results indicate that the Ar-NO_2 surface density can be varied at both LCP and PPS surfaces by regulating the total time or number of cycles in the functionalization reactions. More broadly, this suggests that it is possible to regulate the organic layer thickness

and the coverage of functional groups formed via aryldiazonium functionalization on these polymers.

GATR measurements were carried out also on surfaces modified using the ABA precursor however the relatively weaker cross section of stretching modes associated with COOH/COO^- peaks make it challenging to discriminate the contributions arising from the functional organic layer from those of the polymeric substrate (see Figure S2). Therefore, to confirm functionalization with ABA moieties, the water contact angle of the polymer substrates was monitored instead, given that Ar-COOH surface groups increase wettability. Figure 3d shows water contact angle results obtained on LCP and PPS before and after surface modification using 15 mM aqueous solutions of diazotized ABA containing 0.15 M hypophosphite and 5 mM Cu^{+2} (1 h reactions). The decrease in contact angle supports the formation of a hydrophilic functional layer that is consistent with the presence of Ar-COOH groups. Finally, it is useful to note that the functionalization process does not lead to discoloration or visible degradation of the polymer substrates (see Figure S3) thus confirming that the modification protocol is relatively mild and preserves the appearance and bulk integrity of the materials.

Electroless deposition on pristine and functionalized polymers

The effect of surface modifications on the catalytic activation of polymer surfaces prior to electroless deposition was investigated by focusing on LCP as a diagnostic substrate. The composition and loading of catalytic seeds was quantitated using XPS; Figure 4a shows survey spectra of bare LCP and of LCP-ABA surfaces after sensitization/activation in Sn^{2+}/Pd^{2+} solutions in the 600-250 eV region; LCP-ABA surfaces prepared using one, two and three cycles of 1 h functionalization reactions with diazotized ABA were tested. All spectra show the characteristic C 1s (285 eV) peak associated with the polymer substrate, and peaks associated

with Sn 3d (484 eV) and Pd 3d (335 eV) emissions, thus confirming successful sensitization/activation with Sn/Pd catalytic seeds [1]. The peak at *ca.* 532 eV is assigned to the O 1s peak; however, this peak overlaps with Pd 3p ionizations and was therefore omitted from further analysis. Also, the peak at *ca.* 270 eV is assigned to Cl 2s emissions, arising from chlorides in the functionalization and/or sensitization activation steps.

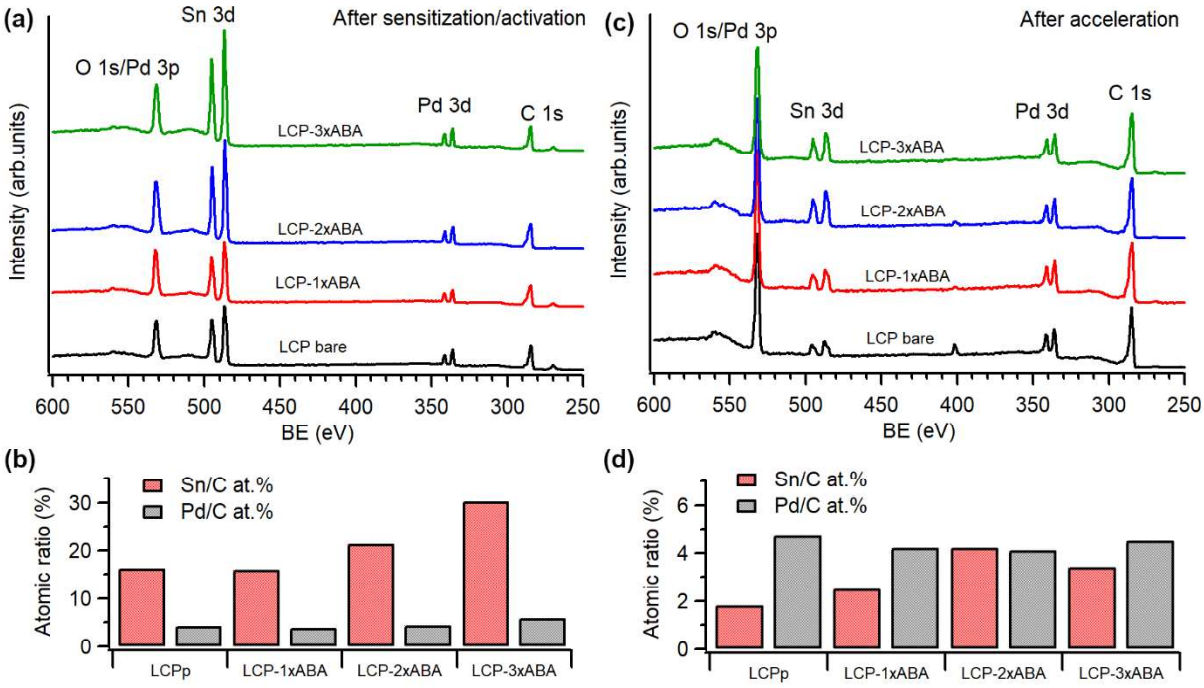

Figure 4. (a) Survey XPS spectra of polished LCP (LCP bare) and of LCP after 1, 2 and 3 cycles of functionalization reactions with diazotized ABA (LCP-#xABA) after undergoing sensitization/activation in Sn^{2+}/Pd^{2+} solutions. (b) Metal loading expressed in M/C atomic %-ratios as a function of surface coverage of -ArCOOH groups calculated from surveys. (c) Survey XPS spectra of surfaces prepared as in (a) after undergoing acceleration. (d) Metal loading expressed in M/C atomic %-ratios obtained after acceleration treatments.

Table 1. Summary of atomic %-composition obtained from XPS spectra; values were calculated from peak area ratios corrected by relative sensitivity factors.

	After sensitization/activation			**After acceleration**		
	Sn/C at.%	**Pd/C at.%**	**M_{tot}/C at.%**	**Sn/C at.%**	**Pd/C at.%**	**M_{tot}/C at.%**
LCPp bare	16.2%	4.3%	20.6%	1.8%	4.7%	6.6%
LCP-1xABA	16.0%	3.8%	19.8%	2.5%	4.2%	6.7%
LCP-2xABA	21.3%	4.4%	25.8%	4.2%	4.1%	8.3%
LCP-3xABA	30.2%	5.9%	36.1%	3.4%	4.5%	7.9%

The surveys indicate that the total metal loading increases with the number of functionalization cycles as evidenced by the increased intensity of the Sn 3d peak. Figure 4b shows the trend in Sn/C and Pd/C atomic %-ratios measured from peak areas in the survey spectra (see Table 1). Results indicate that both Sn and Pd loadings are affected by the surface coverage of Ar-COOH groups; relative to the bare surface, Sn and Pd loadings were increased by up to 90% and 40%, respectively, by repeating the functionalization protocol 3 times. Figure 4c shows the corresponding surveys after acceleration. Spectra confirm that the acceleration step preferentially removes Sn, as indicated by the significantly reduced intensity of the Sn 3d peak relative to the C 1s peak, and in agreement with the main objectives of the treatment [1]. Figure 4d shows the trend in Sn/C and Pd/C atomic %-ratios for the four surfaces which indicate that the Pd/C loading on accelerated surfaces remains close to an average of 4.4%; however, the total amount of Sn goes through a maximum after two cycles of functionalization (see Table 1). These results suggest that the most significant effect of surface Ar-COOH groups is that of increasing binding of Sn(II) species in the sensitization/activation bath, which also translates into increased Sn loading at surfaces after acceleration. Finally, SEM images of LCP surfaces, Figure 5, after sensitization and activation via immersion in the commercial Sn^{2+}/Pd^{2+} solution confirmed nanoparticle formation. The images show evidence of nanoparticles, distributed across the polymer surfaces, consistent with surface decoration with Pd^0/Sn^0 seeds required for electroless deposition [1].

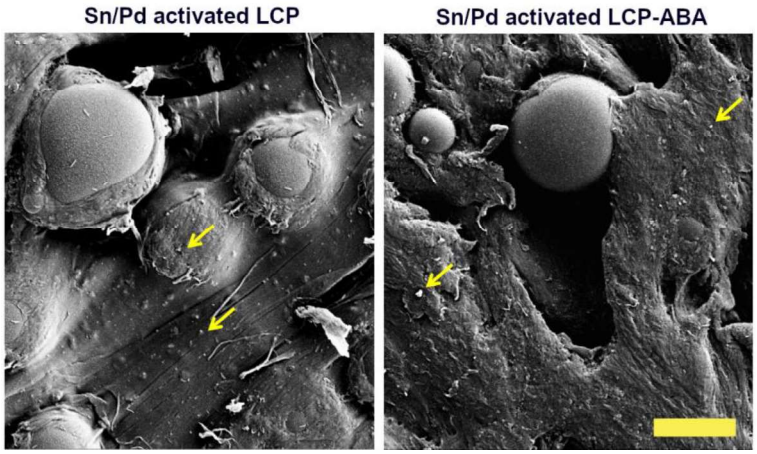

Figure 5. SEM images of polished LCP (left) and of LCP after functionalization reactions with diazotized ABA (right) after undergoing sensitization/activation in Sn^{2+}/Pd^{2+} solutions; scalebar = 10 µm; arrows indicate examples of locations at which metal nanoparticles are discernible.

Adhesion strength studies on electrolessly deposited copper

The effect of surface modifications on the adhesion strength of electrolessly deposited metal films was investigated using peel tests at 180°. Figure 6a shows a summary of copper adhesion strength results for LCP-ABA surfaces prepared using one, two and three cycles of 1 h functionalization reactions with diazotized ABA. The results are compared to those obtained on copper films deposited directly onto bare LCP surfaces (i.e. non-functionalized), and on aggressively sanded LCP surfaces. The figure displays the distribution of adhesion strength values and box and whisker plots; numerical values are also reported in Table 2. Results for sanded LCP surfaces show a median of 1.28 N/mm and a short tail at low adhesion strengths; these values reflect the maximum adhesion strength rating of the test tape on the Cu surface and, in fact, no significant peeling of the Cu film was observed on sanded LCP coupons. Results for bare LCP, show that in the absence of functionalization or aggressive roughening the copper film displays extremely poor adhesion with a median value ca. 0.1 N/mm. All LCP-ABA

surfaces yielded significantly higher adhesion strengths of the metallized copper layer relative to the bare polymer, with median values that are indistinguishable from those of sanded LCP.

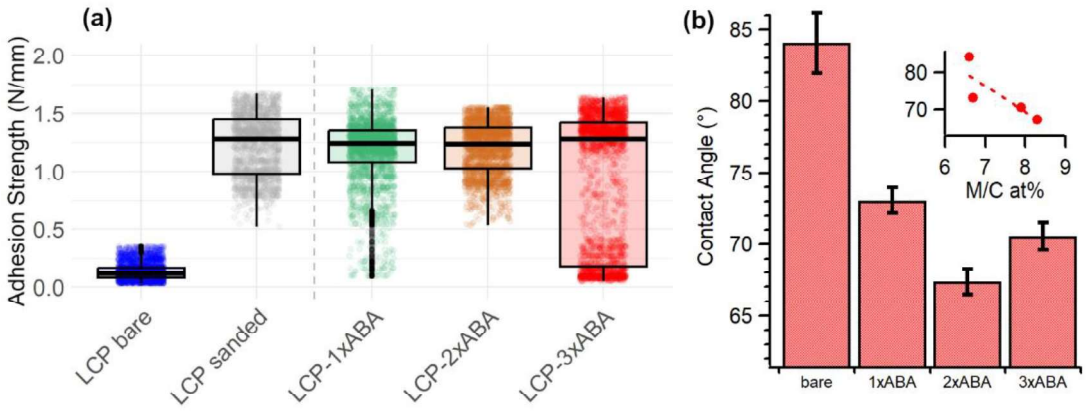

Figure 6. (a) Adhesion strength values obtained from measurements of 180° peel tests on copper plated coupons of LCP (N =3). Results compare the adhesion strength of electrolessly deposited layers on LCP modified with Ar-COOH groups via one, two, three and 4 cycles of 1 h reactions with diazotized ABA. Results are compared to those obtained on unmodified (bare) LCP and on a high adhesion control sample obtained by sanding the surface with P1200 grit paper. (b) Water contact angle of LCP surfaces pre-treated under the same conditions as those used in panel (a).

Table 2. Summary of adhesion strength values and statistics for metal films electrolessly deposited on samples described in Table 2.

Sample	Median (N/mm)	75% (3rd Q) (N/mm)	25% (1st Q) (N/mm)
LCP-1xABA	1.24	1.35	1.08
LCP-2xABA	1.24	1.38	1.03
LCP-3xABA	1.28	1.42	0.18
LCP-bare	0.12	0.17	0.08
LCP-sanded	1.28	1.45	0.98
LCP-pNBD	0.42	1.10	0.29
PPS-1xABA	0.73	0.98	0.46
PPS-3xABA	1.15	1.28	0.22
PPS bare	0.13	0.29	0.10
PPS sanded	1.29	1.67	0.99

It is interesting to note that the distribution of adhesion strength values in Figure 6a is strongly affected by the number of functionalization cycles and, therefore, by the

coverage/morphology of the carboxyphenyl organic layer. Both LCP-1xABA and LCP-2xABA coupons yielded median and 1st quartile values above the 1 N/mm benchmark point. Longer functionalization protocols, however, are not beneficial and result in the appearance of regions of low adhesion over the surface of the LCP coupons, as evidenced by subpopulations with local maxima in the distribution at values <0.5 N/mm. LCP-2xABA samples yielded the best results in this series, as they display a narrow distribution in the measured adhesion strength, with the minimum whisker at ca. 0.5 N/mm. This result suggests that the copper adhesion strength is sensitive to the coverage/density of carboxyphenyl groups and that this can be optimised to achieve values that are comparable to those observed with the aggressively sanded LCP surfaces.

Further support for this was obtained from water contact angle measurements of LCP coupons pre-treated under the same conditions as those used for the electroless deposition, as shown in Figure 6b. The contact angle was observed to decrease after one and two cycles of functionalization; however, the third cycle yields an increase indicating lower availability of hydrophilic groups at the LCP interface. Interestingly, the water contact angle results (see inset) are negatively correlated to the density of catalytic seeds after acceleration summarized in Table 1. These results therefore support the idea that the coverage of free surface-bound -COOH groups, for which wettability is diagnostic, results in higher catalytic seed loadings and higher adhesion strengths. Multiple functionalization cycles can thus be beneficial because they increase coverage; however, once disordered multilayers are formed, it is likely that oligomerization takes place more readily via reactions at the -COOH sites, rather than at the *o*-positions of the aryl rings alone (cf. Figure 1b).

To probe whether the enhanced adhesion resulted from the presence of specific chemical interactions with -COOH groups rather than from other reactions taking place during functionalization, the adhesion strength was also measured for LCP coupons modified with nitrophenyl groups. Table 2 shows copper adhesion strength values obtained after 1 cycle of functionalization using pNBD (LCP-pNBD). Although functionalization with nitrophenyl groups results in a marginal improvement of the Cu adhesion strength, the median value remains low at 0.42 N/mm, while the results obtained after 1 h of functionalization with carboxyphenyl groups are significantly better. This indicates that specific interactions with Ar-COOH groups play an important role in the improved adhesion.

Finally, enhancements in the adhesion strength were also observed in the case of PPS. Figure 7 shows adhesion strengths obtained for copper films deposited on bare PPS and on PPS modified with one and three 1 h-cycles of functionalization with diazotized ABA; control results obtained with sanded PPS surfaces are also shown for comparison. Bare PPS surfaces yielded poor adhesion of the copper film, with a median value of ca. 0.1 N/mm. PPS-1xABA and PPS-3xABA both yielded significantly higher adhesion strengths with three cycles performing better in terms of both median strength and homogeneity.

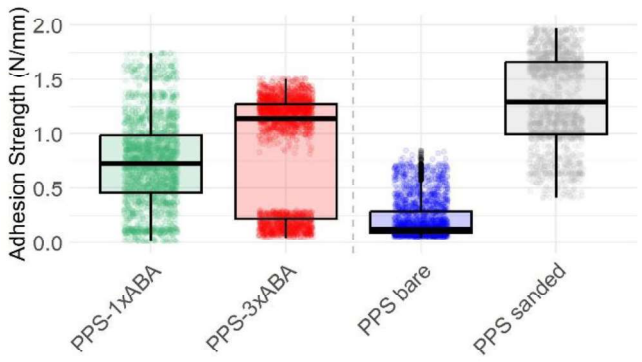

Figure 7. Adhesion strength values obtained from measurements on replicate coupons (N=3) of bare PPS and of PPS after functionalization via one and three cycles of 1 h reactions with diazotized ABA; the high adhesion control obtained via sanding with P1200 grit paper is also shown for comparison.

It is important to note that improvements in copper adhesion observed in Figure 6 are achieved without increasing the roughness of the polymer surface. This was demonstrated by determinations of the rms roughness (R_q) via profilometry on LCP surfaces. Figure 8 shows R_q determinations on the LCP surfaces before and after deposition of the copper films, in the case of bare LCP, sanded LCP and LCP-2xABA, i.e. the best performer in terms of adhesion strength; the R_q value of as received polymers is shown with a dashed line. Results indicate that neither the mechanical cleaning, nor the functionalization with carboxyphenylene layers results in increased roughness, as the mean R_q remains below that of the as received polymer. On the other hand, the enhanced adhesion strength that results from sanding pre-treatments is obtained at the expense of a significant increase in roughness. Interestingly, the mean roughness of the metal film was the lowest on functionalized surfaces thus indicating that the carboxyphenylene layers might improve not only adhesion but also the roughness of final metallized polymers.

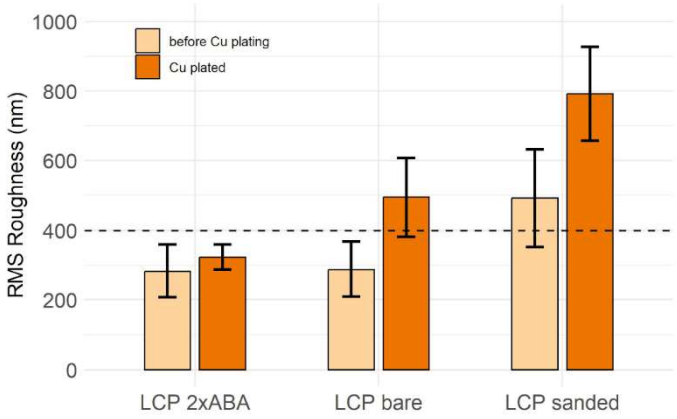

Figure 8. RMS roughness (R_q) values measured via profilometry at LCP-2xABA, LCP bare and LCP sanded surfaces before and after electroless deposition of Cu layers. The R_q value of the LCP polymer coupons as received is shown with a dashed line to facilitate comparison.

The above results show that surface immobilization of carboxyphenylene groups results in improved adhesion of electrolessly deposited copper without any significant roughening. The role of functional groups at pre-treated polymer surfaces has received significant attention in the electroless deposition literature; however, the specific role of such functionalities remains under debate, as recently discussed [45]. The increases observed in both wettability and catalyst density upon functionalization with our ArCOOH layers are consistent with the existing literature on the impact of surface functionalities. Improved adhesion of metal films has been attributed to improved wettability after modification with a range of polar groups such as pyridinic [46], pyrrolic [47] and hydroxyl/carboxyl moieties [48]. Wettability effects are likely to play a role also in the case of ArCOOH adlayers from aryldiazonium cations, given that trends in contact angle vs number of functionalization cycles parallel trends in adhesion strength. Functional organic layers based on e.g. pyridinic-N [46, 49, 50] or carboxylates [12, 18] have been argued to promote chemisorption of catalytic metal seeds through either electrostatic or Lewis acid-base interactions; however, the effects of molecular coverage on catalyst loading have received limited attention. Most studies of COOH functionalities rely on oxidative processes, making it challenging to separate the keying effect of roughening from that of chemisorptive interactions [45]. The strategy adopted by Palacin and co-workers [18] using grafted PAA polymer brushes at non-roughened ABS is an interesting exception. Their results strongly suggest that a high surface density of COOH groups is indeed desirable for high adhesion; nonetheless, metal interlocking within the nanoscale brush film (<15 nm) was still considered to play a role in their work, in synergy with the increased density of metal catalyst. This is further supported conclusions from recent studies by Lubineau and co-workers that suggest that mechanical interlocking plays a much more important role than chemical interactions [45, 51]. Given that changes in polymer substrate topography are

avoided under the very mild conditions used for aryldiazonium grafting, we propose that a keying effect, similar to that observed with PAA brushes, could be at play as the result of ArCOOH multilayer formation. Importantly, the protocol presented herein offers a lower level of complexity than most grafting-on/-from strategies involving polymer brushes, thus making it of potential relevance for implementations at scale.

Conclusions

In this work we investigated the application of functional organic films consisting of carboxyphenylene moieties grafted using 4-carboxybenzene diazonium cations to improve the adhesion strength of metal films deposited on polymer substrates. We first show that Ar-COOH films can be covalently grafted onto LCP and PPS polymers, two materials of the family of super-engineering plastics that are considered as high-performing for a range of applications. The functionalization requires use of a reductant in solution together with small amounts of a metal salt to promote dediazoniation.

Adhesion strength determinations on metallized polymers showed that Ar-COOH functional layers grafted via reactions with aryldiazonium cations improve adhesion of the metal. Control experiments using nitrophenyl groups suggest that the specific choice of functional group has a profound effect on the adhesion strength. The coverage of the ArCOOH film can be optimized by controlling the duration of the grafting reactions; coverage and likely multilayer formation appears to positively correlate with the binding and loading of Pd/Sn nanoparticles used to catalyse the electroless copper deposition at the polymer surface.

Interestingly, functionalization with the best performing Ar-COOH layers has negligible effects on the surface roughness of LCP coupons and of the copper film ultimately obtained after the

electroless deposition. The structural integrity of the polymer can be assured throughout the procedure given the absence of a roughening step, the mild conditions used for the surface modification and the use of aqueous solutions, as these do not result in swelling or loss of dimensionality. Results therefore show that both chemical adhesion and organic film morphology might play an important role and can be tailored to deliver performances comparable to more aggressive methods without any degradation in polymer topography. Therefore, these aryldiazonium reactions open the door to applications of this method to the fabrication of ultra-smooth metallized polymer substrates and/or of complex metallized features with e.g. high aspect ratio and 3D architectures.

Acknowledgements

Part of this publication has emanated from research conducted with the financial support of Science Foundation Ireland under Grant No. 19/FFP/6761. Use of the XPS of I. V. Shvets and C. McGuinness provided under SFI Equipment Infrastructure funds. SEM imaging was carried out at the Advanced Microscopy Laboratory (AML) at the AMBER Research Centre, Trinity College Dublin, Ireland. The authors gratefully acknowledge Dr. Mohammad Divandari for useful feedback and discussions.

References

[1] X. Wei, D.K. Roper, Tin Sensitization for Electroless Plating Review, J. Electrochem. Soc., 161 (2014) D235-D242.

[2] G.O. Mallory, J.B. Hajdu, Electroless Plating - Fundamentals and Applications, William Andrew Publishing/Noyes 1990.

[3] J. Kim, S.H. Wen, D.Y. Jung, R.W. Johnson, Microstructure evolution during electroless copper deposition, IBM Journal of Research and Development, 28 (1984) 697-710.

[4] G.O. Mallory, J.B. Hajdu, Plating on Plastics, Electroless Plating - Fundamentals and Applications, William Andrew Publishing/Noyes1990, pp. 377-399.

[5] R. Sard, The Nucleation, Growth, and Structure of Electroless Copper Deposits, J. Electrochem. Soc., 117 (1970) 864.

[6] N. Feldstein, P.R. Amodio, Anionic Inhibition in Electroless Plating, J. Electrochem. Soc., 117 (1970) 1110.

[7] P. Doppelt, G. Hallais, J. Pinson, F. Podvorica, S. Verneyre, Surface Modification of Conducting Substrates. Existence of Azo Bonds in the Structure of Organic Layers Obtained from Diazonium Salts, Chem. Mater., 19 (2007) 4570-4575.

[8] G.R. Logie, A. Rantell, The Adhesion of Electroless Metal Deposits to A B S and other Polymers, Transactions of the IMF, 46 (1968) 91-94.

[9] R.G. Wedel, Durability and structure of electroplated plastics, International Metals Reviews, 22 (1977) 97-118.

[10] R. Melentiev, R. Tao, X. Li, A.K. Tevtia, N. Verghese, G. Lubineau, Mapping the coating failure modes of electroless plated metal on ABS polymer with micro-nano structured interface, Int. J. Adhes. Adhes., 126 (2023) 103471.

[11] A. Rantell, The Influence of Surface Chemistry on the Adhesion of Copper Deposited on Plastic Substrates, Transactions of the IMF, 47 (1969) 197-202.

[12] K.M. Metz, P.E. Colavita, K.-Y. Tse, R.J. Hamers, Nanotextured gold coatings on carbon nanofiber scaffolds as ultrahigh surface-area electrodes, J. Power Sources, 198 (2012) 393-401.

[13] K.M. Metz, D. Goel, R.J. Hamers, Molecular Monolayers Enhance the Formation of Electrocatalytic Platinum Nanoparticles on Vertically Aligned Carbon Nanofiber Scaffolds, J. Phys. Chem. C, 111 (2007) 7260-7265.

[14] K.M. Metz, K.-Y. Tse, S.E. Baker, E.C. Landis, R.J. Hamers, Ultrahigh-Surface-Area Metallic Electrodes by Templated Electroless Deposition on Functionalized Carbon Nanofiber Scaffolds, Chem. Mater., 18 (2006) 5398-5400.

[15] D. Aldakov, Y. Bonnassieux, B. Geffroy, S. Palacin, Selective Electroless Copper Deposition on Self-Assembled Dithiol Monolayers, ACS Appl. Mater. Inter., 1 (2009) 584-589.

[16] S. Sawada, Y. Masuda, P. Zhu, K. Koumoto, Micropatterning of Copper on a Poly(ethylene terephthalate) Substrate Modified with a Self-Assembled Monolayer, Langmuir, 22 (2006) 332-337.

[17] P. Li, Y. Zhang, Z. Zheng, Polymer-Assisted Metal Deposition (PAMD) for Flexible and Wearable Electronics: Principle, Materials, Printing, and Devices, Adv. Mater., 31 (2019) 1902987.

[18] A. Garcia, T. Berthelot, P. Viel, A. Mesnage, P. Jégou, F. Nekelson, S. Roussel, S. Palacin, ABS Polymer Electroless Plating through a One-Step Poly(acrylic acid) Covalent Grafting, ACS Appl. Mater. Inter., 2 (2010) 1177-1183.

[19] R.J. Cullen, D.R. Jayasundara, R.J. Baker, G. O' Connell, T. Donnelly, K.E. Ballantine, J.G. Lunney, P.E. Colavita, Laser-driven rapid functionalization of carbon surfaces and its application to the fabrication of fluorinated adsorbers, RSC Adv., 6 (2016) 82924-82932.

[20] P.E. Colavita, B. Sun, K.-Y. Tse, R.J. Hamers, Photochemical Grafting of n-Alkenes onto Carbon Surfaces: the Role of Photoelectron Ejection, Journal of the American Chemical Society, 129 (2007) 13554-13565.

[21] D.K. Platt, R.T. Limited, Engineering and High Performance Plastics Market Report: A Rapra Market Report, Rapra Technology Limited 2003.

[22] T. Breton, A.J. Downard, Controlling Grafting from Aryldiazonium Salts: A Review of Methods for the Preparation of Monolayers, Aust. J. Chem., 70 (2017) 960-972.

[23] T. Menanteau, M. Dias, E. Levillain, A.J. Downard, T. Breton, Electrografting via Diazonium Chemistry: The Key Role of the Aryl Substituent in the Layer Growth Mechanism, J. Phys. Chem. C, 120 (2016) 4423-4429.

[24] T. Menanteau, E. Levillain, T. Breton, Electrografting via Diazonium Chemistry: From Multilayer to Monolayer Using Radical Scavenger, Chem. Mater., 25 (2013) 2905-2909.

[25] M.D. Angione, T. Duff, A.P. Bell, S.N. Stamatin, C. Fay, D. Diamond, E.M. Scanlan, P.E. Colavita, Enhanced antifouling properties of carbohydrate coated poly(ether sulfone) membranes, ACS Appl. Mater. Inter., 7 (2015) 17238–17246.

[26] J.A. Behan, A. Myles, A. Iannaci, É. Whelan, E.M. Scanlan, P.E. Colavita, Bioinspired electro-permeable glycans on carbon: Fouling control for sensing in complex matrices, Carbon, 158 (2020) 519-526.

[27] V.R. Sastri, Chapter 8 - High-Temperature Engineering Thermoplastics: Polysulfones, Polyimides, Polysulfides, Polyketones, Liquid Crystalline Polymers, and Fluoropolymers, in: V.R. Sastri (Ed.) Plastics in Medical Devices, William Andrew Publishing, Boston, 2010, pp. 175-215.

[28] G. Socrates, Infrared and Raman Characteristic Group Frequencies: Tables and Charts, Wiley 2004.

[29] Y. Liu, Y. Liu, H. Tan, C. Wang, H. Wei, Z. Guo, Structural evolution and degradation mechanism of Vectran® fibers upon exposure to UV-radiation, Polym. Degrad. Stab., 98 (2013) 1744-1753.

[30] L. Esteban-Tejeda, T. Duff, G. Ciapetti, M. Daniela Angione, A. Myles, J.M. Vasconcelos, E.M. Scanlan, P.E. Colavita, Stable hydrophilic poly(dimethylsiloxane) via glycan surface functionalization, Polymer, 106 (2016) 1-7.

[31] A. Myles, D. Haberlin, L. Esteban-Tejeda, M.D. Angione, M.P. Browne, M.K. Hoque, T.K. Doyle, E.M. Scanlan, P.E. Colavita, Bioinspired Aryldiazonium Carbohydrate Coatings: Reduced Adhesion of Foulants at Polymer and Stainless Steel Surfaces in a Marine Environment, ACS Sus. Chem. Eng., 6 (2018) 1141-1151.

[32] R.J. Cullen, D. Jayasundara, L. Soldi, J. Cheng, G. DuFaure, P.E. Colavita, Spontaneous grafting of nitrophenyl groups on amorphous carbon thin films: A structure-reactivity investigation, Chem. Mater., 24 (2012) 1031–1040.

[33] D. Jayasundara, R.J. Cullen, P.E. Colavita, In situ and real time characterization of spontaneous grafting of aryldiazonium salts at carbon surfaces, Chem. Mater., 25 (2013) 1144–1152.

[34] B.M. Simons, J. Lehr, D.J. Garrett, A.J. Downard, Formation of Thick Aminophenyl Films from Aminobenzenediazonium Ion in the Absence of a Reduction Source, Langmuir, 30 (2014) 4989-4996.

[35] M. Picot, R. Rodulfo, I. Nicolas, A. Szymczyk, F. Barrière, M. Rabiller-Baudry, A versatile route to modify polyethersulfone membranes by chemical reduction of aryldiazonium salts, J. Membr. Sci., 417-418 (2012) 131-136.

[36] M.M. Chehimi, A. Lamouri, M. Picot, J. Pinson, Surface modification of polymers by reduction of diazonium salts: polymethylmethacrylate as an example, J Mater Chem C, 2 (2014) 356-363.

[37] V. Mévellec, S. Roussel, L. Tessier, J. Chancolon, M. Mayne-L'Hermite, G. Deniau, P. Viel, S. Palacin, Grafting Polymers on Surfaces: A New Powerful and Versatile Diazonium Salt-Based One-Step Process in Aqueous Media, Chem. Mater., 19 (2007) 6323-6330.

[38] H. Yan, A.J. Bergren, R. McCreery, M.L. Della Rocca, P. Martin, P. Lafarge, J.C. Lacroix, Activationless charge transport across 4.5 to 22 nm in molecular electronic junctions, Proc. Nat. Ac. Sci., 110 (2013) 5326-5330.

[39] J. Pinson, F. Podvorica, Attachment of organic layers to conductive or semiconductive surfaces by reduction of diazonium salts, Chem. Soc. Rev., 34 (2005) 429-439.

[40] P. Abiman, G.G. Wildgoose, R.G. Compton, Investigating the Mechanism for the Covalent Chemical Modification of Multiwalled Carbon Nanotubes Using Aryl Diazonium Salts, Int. J. Electrochem. Sci., 3 (2008) 104-117.

[41] CRC Handbook of Chemistry and Physics, CRC Press 1998.

[42] D. Li, Y. Luo, D. Onidas, L. He, M. Jin, F. Gazeau, J. Pinson, C. Mangeney, Surface functionalization of nanomaterials by aryl diazonium salts for biomedical sciences, Adv. Colloid Interface Sci., 294 (2021) 102479.

[43] L. Fensterbank, J.-P. Goddard, M. Malacria, C. Ollivier, Homolytic Reduction of Onium Salts, CHIMIA, 66 (2012) 425.

[44] C. Guyon, E. Métay, F. Popowycz, M. Lemaire, Synthetic applications of hypophosphite derivatives in reduction, Organic & Biomolecular Chemistry, 13 (2015) 7879-7906.

[45] R. Tao, L. Fatta, R. Melentiev, A.K. Tevtia, G. Lubineau, Contributions of chemical interactions and mechanical interlocking for the adhesion of electroplated copper to ABS in the Cr(VI) etching process, Int. J. Adhes. Adhes., 126 (2023) 103450.

[46] N.P. Vu, X.T. Duong, V.A. Ly, D.C. Nguyen, M.D. Tran, Q.T. Phan, M. Balazinski, L.T. Son, G. Zeb, X.T. Le, Electroless nickel plating onto Plexiglas® through simple covalent grafting of vinylpyridine seed layer, Materials & Design, 144 (2018) 151-158.

[47] M. Bazzaoui, J.I. Martins, E.A. Bazzaoui, A. Albourine, R. Wang, P.-D. Hong, A simple method for acrylonitrile butadiene styrene metallization, Surf. Coat. Technol., 224 (2013) 71-76.

[48] Z. Li, N. Li, L. Yin, Y. He, Z. Wang, An Environment-Friendly Surface Pretreatment of ABS Resin Prior to Electroless Plating, Electrochem. Solid-State Lett., 12 (2009) D92.

[49] D. Xu, E.T. Kang, K.G. Neoh, Y. Zhang, A.A.O. Tay, S.S. Ang, M.C.Y. Lo, K. Vaidyanathan, Selective Electroless Plating of Copper on (100)-Oriented Single Crystal Silicon Surface Modified by UV-Induced Coupling of 4-Vinylpyridine with the H-Terminated Silicon, The Journal of Physical Chemistry B, 106 (2002) 12508-12516.

[50] T.J. Bradley, W.C.E. Schofield, R.P. Garrod, J.P.S. Badyal, Electroless Metallization onto Pulsed Plasma Deposited Poly(4-vinylpyridine) Surfaces, Langmuir, 22 (2006) 7552-7555.

[51] A. Yudhanto, X. Li, R. Tao, R. Melentiev, G. Lubineau, Identifying adhesion characteristics of metal-polymer interfaces: Recent advances in the case of electroplated acrylonitrile butadiene styrene, Materials Today Communications, 35 (2023) 106218.